DOI: 10.1002/asia.200600182

Halide-Anion Binding by Singly and Doubly N-Confused Porphyrins

Hiromitsu Maeda,[b] Tatsuki Morimoto,[a] Atsuhiro Osuka,[c] and Hiroyuki Furuta*[a, d]

Abstract: The halide-binding properties of N-confused porphyrin (NCP, **1**) and doubly N-confused porphyrins (*trans*-N_2CP (**2**), *cis*-N_2CP (**3**)) were examined in CH_2Cl_2. In the free-base forms, *cis*-N_2CP (**3**) showed the highest affinity to each anion (Cl^-, Br^-, I^-) with association constants $K_a = 7.8 \times 10^3$, 1.9×10^3, and $5.8 \times 10^2\ M^{-1}$, respectively. As metal complexes, on the other hand, *trans*-N_2CP **2–Cu** exhibited the highest affinity to Cl^-, Br^-, and I^- with $K_a = 9.0 \times 10^4$, 2.7×10^4, and $1.9 \times 10^3\ M^{-1}$, respectively. The corresponding K_a values for *cis*-N_2CP **3–Cu** and NCP **1–Cu** were about 1/10 and 1/2, respectively, of those of **2–Cu**. With the help of density functional theory (DFT) calculations and complementary affinity measurements of a series of trisubstituted N-confused porphyrins, the efficient anion binding of NCPs was attributed to strong hydrogen bonding at the highly polarized NH moieties owing to the electron-deficient C_6F_5 groups at *meso* positions as well as the ideally oriented dipole moments and large molecular polarizability. The orientation and magnitude of the dipole moments in NCPs were suggested to be important factors in the differentiation of the affinity for anions.

Keywords: anions · binding studies · N-confused porphyrins · pi interactions · porphyrinoids

Introduction

Anion binding by artificial molecules has attracted considerable attention in recent years with the expectation for anion sensors, transporters, catalysts, and so on.[1] In designing artificial anion receptors, a multipoint binding strategy is usually applied to increase the affinity for target anions.[2–5] For example, oligopyrrole macrocycles were shown to bind anions highly efficiently through multiple hydrogen bonding with preorganized pyrrole NH groups. Sessler and co-workers reported calix[4]pyrrole, a neutral oligopyrrole macrocycle that captures F^- and Cl^- in the cavity at four points by binding through hydrogen bonding with the tetrapyrrole NH moieties,[4] and diprotonated sapphyrin, a cationic pentapyrrole expanded porphyrin that binds F^- strongly by five-point hydrogen bonding in combination with electrostatic interactions.[5] In both cases, pyrrole NH groups serve as hydrogen-bonding donors to anions. In the case of porphyrins, on the other hand, the NH groups are usually less active towards anions because the size of the inner core is too small to trap the anions inside, and the molecules resist distortion to maintain the planarity owing to the large aromatic stabilization. Once porphyrins form metal complexes, however, the anions are likely to coordinate to the central metal as axial ligands, and anion-exchange reactions could be used to coordinate certain anions.[6]

For a decade, we and others have been studying N-confused porphyrins (NCP) and related compounds and revealed a variety of properties attributed to the confused pyrrole ring(s) in the macrocycles.[7,8] In the tetrapyrrole framework, the N or NH atoms of the confused pyrrole ring(s) are located at the periphery, and thus those atoms can interact with hydrogen-bonding donors, acceptors, or metals

[a] T. Morimoto, Prof. Dr. H. Furuta
Department of Chemistry and Biochemistry
Graduate School of Engineering
Kyushu University
Fukuoka 819-0395 (Japan)
Fax: (+81) 92-802-2865
E-mail: hfuruta@cstf.kyushu-u.ac.jp

[b] Prof. Dr. H. Maeda
Department of Bioscience and Biotechnology
Faculty of Science and Engineering
Ritsumeikan University
Kusatsu 525-8577 (Japan)

[c] Prof. Dr. A. Osuka
Department of Chemistry
Graduate School of Science
Kyoto University
Kyoto 606-8502 (Japan)

[d] Prof. Dr. H. Furuta
PRESTO
Japan Science and Technology Agency (JST)
Kawaguchi 332-0012 (Japan)

Supporting information for this article is available on the WWW under http://www.chemasianj.org or from the author.

easily.[8] Recently, we reported a peculiar anion-binding property of C_6F_5-substituted N-confused porphyrin metal complexes **1–M** (Figure 1).[9,10] In this system, significantly

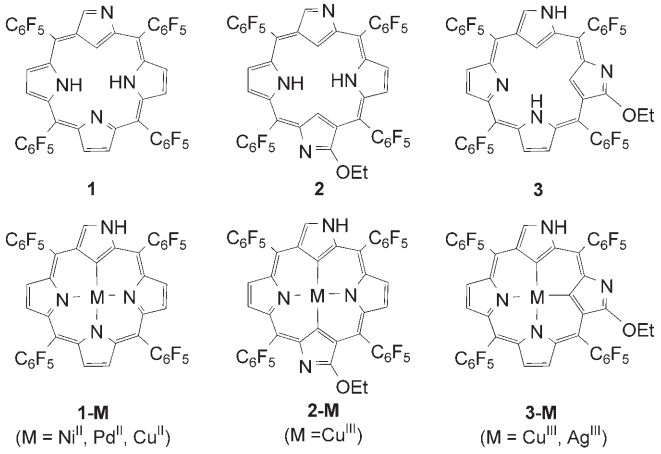

Figure 1. Free bases and metal complexes of NCP **1**, *trans*-N_2CP **2**, and *cis*-N_2CP **3**.

high affinity to Cl^-, Br^-, and I^- was observed, and these anions were suggested to be located at the peripheral NH group through hydrogen bonding (Scheme 1).[9] To understand this type of binding further, we have studied the anion-binding properties of three kinds of N-confused porphyrinoids **1** and *trans*- and *cis*-types of doubly N-confused porphyrins (*trans*-N_2CP (**2**) and *cis*-N_2CP (**3**)) in the free-base and the metal-complex forms (Figure 1).[10–12] The N_2CPs bear hydrogen-bonding donor (NH) and acceptor (N) atoms at the periphery. Just like imidazole,[13] they interact with each other to form 1D hydrogen-bonding networks in the solid state.[11,12d] From the arrangement of NH groups at the periphery of N_2CPs, anion-binding properties similar to those of NCPs could be anticipated. Interestingly, the affinity for halide anions differed largely among three porphyrinoids, and the Cu^{III} complex of *trans*-N_2CP, **2–Cu**, exhibited the highest affinity. Herein we report details of the anion-binding properties of NCPs and N_2CPs, and discuss the factors that control the present anion-binding system with the help of density functional theory (DFT) calculations as well as the complementary affinity measurements of a series of trisubstituted N-confused porphyrins. The obtained data indicate that the anion binding of **1–3** occurs at the peripheral NH groups through hydrogen-bonding interactions, and the presumed anion–π interactions between the anion and the neighboring electron-deficient aromatic ring is negligible.[14] In addition to the existence of hydrogen-bonding donor sites at the periphery, inductive effects of *meso*-C_6F_5 groups, ion–dipole interactions, which depend on the magnitude and orientation of the dipole moments of N-confused porphyrinoids, and ion–induced dipole interactions, which are related to the polarizability of large π-ring systems, are suggested to be significant in determining the anion-binding affinity of NCPs and N_2CPs.[15]

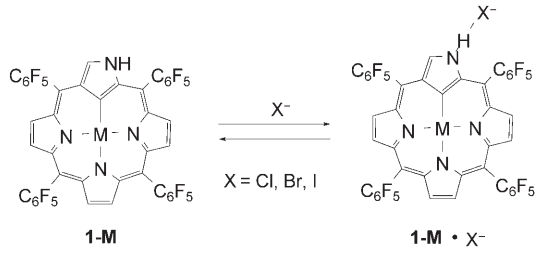

Scheme 1. A plausible anion-binding mode of **1–M**.

Abstract in Japanese:

N-混乱ポルフィリン(NCP)および二重N-混乱ポルフィリン(*trans*-, *cis*-N_2CP)のCH_2Cl_2中でのハライドアニオンに対する認識挙動を検証した。フリーベース体では*cis*-N_2CP、金属錯体では*trans*-N_2CP Cu^{III}錯体がハライドアニオンに対して最も高い会合能を示した。一連のポルフィリン異性体の高いアニオン錯形成能は、密度汎関数法による計算と三置換型NCPの認識能を検証した結果、(1) メゾ位のC_6F_5基によって分極した環外周NH部位での水素結合、(2) 双極子モーメントの理想的な配向や大きな分極率、に起因することが明らかとなった。各異性体における双極子モーメントの配向と大きさは、それらのアニオン認識能を決定する重要な要因であることが示唆された。

Results and Discussion

Anion Binding of Free Base NCP and N_2CP

In contrast to normal porphyrins that undergo hydrogen-atom exchange in the macrocyclic core, free base NCPs and N_2CPs utilize both the inner and the peripheral N atoms in NH tautomerism.[16] The tautomeric equilibria depend on the solvent, and the predominant tautomeric forms of **1–3** in CH_2Cl_2 are shown in Figure 1.[17,18] Structurally, the external N atom(s) of the confused pyrrole ring(s) in **1** and **2** are deprotonated (N); on the other hand, in **3**, one of the peripheral N atoms is protonated (NH). These differences affect the aromaticity of each tautomer, because 18π annulene conjugation pathways can be drawn in **1** and **2**, but the circuits are disrupted at the confused pyrrole moiety in **3**.

When tetrabutylammonium chloride was added to solutions of the respective confused porphyrins in CH_2Cl_2, the absorption spectra clearly changed (Figure 2). In the case of **1** and **2**, the intensity of the Soret bands decreased, whereas that of the Q bands increased. On the other hand, bathochromic shifts of the Soret bands and fading of the Q bands were observed for **3**. From the change in the Soret bands upon titration, the association constants K_a of **1–3** for Cl^- were determined to be 5.8×10^2, 2.8×10^3, and $7.8\times10^3\,M^{-1}$, respectively, and smaller K_a values were obtained for Br^- and I^- (Table 1).[19]

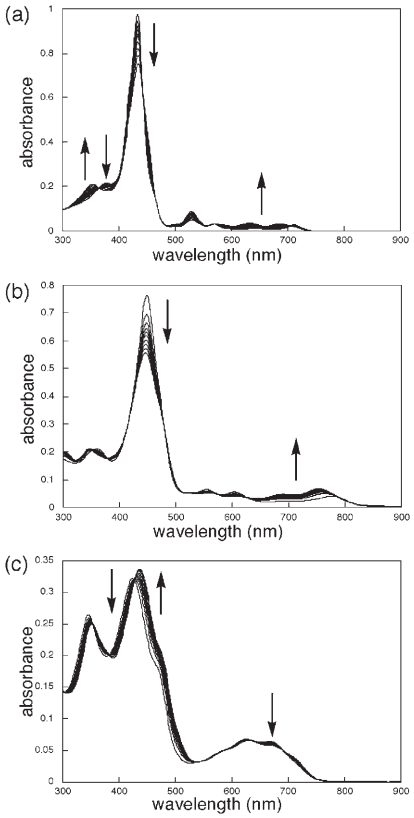

Figure 2. Changes in the absorption spectra of the free-base porphyrins (NCP (**1**), *trans*-N_2CP (**2**), *cis*-N_2CP (**3**)) in CH_2Cl_2 upon the addition of tetrabutylammonium chloride: a) **1** (5.9×10^{-6} M), b) **2** (6.0×10^{-6} M), and c) **3** (6.4×10^{-6} M).

Table 1. Association constants (K_a, M^{-1}) of **1**–**3** for halide anions in CH_2Cl_2.

Anions[a]	1	2	3
Cl^-	5.8×10^2	2.8×10^3	7.8×10^3
Br^-	1.2×10^2	6.3×10^2	1.9×10^3
I^-	40	1.9×10^2	5.8×10^2

[a] Added as tetrabutylammonium salts.

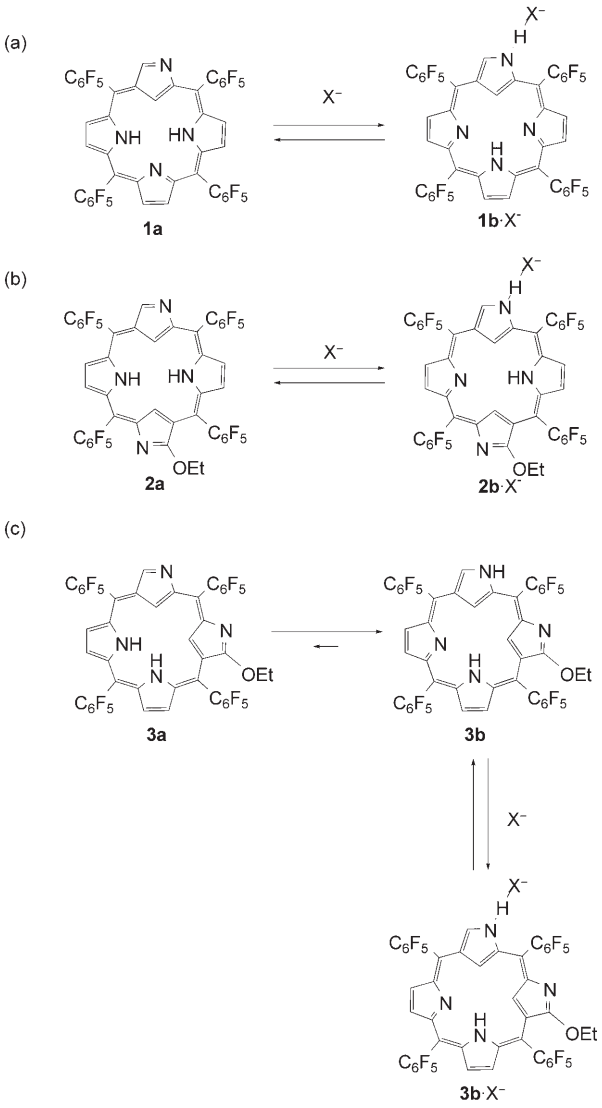

Scheme 2. Tautomeric equilibrium shifts of **1**–**3** upon the addition of anions.

Evidence of the anion-induced NH tautomerism of **1** and **2** was found by ^{1}H NMR analysis. In the absence of anions, only the tautomers **1a** and **2a** were observed in $CDCl_3$, whereas the less-aromatic tautomers **1b** and **2b** were detected in the presence of anions (Scheme 2). In the ^{1}H NMR spectra of **2**, for instance, only the signals of **2a**, which can be seen easily from the resonance of the inner CH proton at $\delta=-4.5$ ppm, were detected in the absence of anions (Figure 3a). Upon the addition of 1 equivalent of Cl^-, the signals assigned to the outer NH of **2b** appeared at $\delta=$ 13.93 ppm along with a decrease in the intensity of the signals of **2a**.[20] Similar tautomeric equilibrium shifts were also observed for **1**. In the case of **3**, however, only the tautomer **3b** was detected under both conditions, although the inner core protons were shifted upfield ($\Delta\delta=-0.97$, -0.98, and -0.99 ppm for CH and two NH protons, respectively) in the presence of Cl^-. Thus the highest binding affinity of **3** may be attributable to the preorganized outer NH group in **3**.

The above anion-binding features were also manifested by fluorescence spectroscopy. Compared with the absorption spectral change, the fluorescence of NCP **1** was remarkably augmented in the presence of anions (Figure 4).[21,22] Similarly, the fluorescence of both *trans*-N_2CP (**2**) and *cis*-N_2CP (**3**) was enhanced; however, the corresponding changes were modest compared to **1**. It is likely that the fluorescence intensity does not differ largely in both tautomers of **2**, and in the case of **3**, the predominant tautomer **3b** has an outer NH group, so it can bind anions without causing shifts in the tautomeric equilibrium. The large enhancement in the fluorescence intensity in the presence of Cl^- would make the free base NCP **1** attractive as a fluorescence sensor for Cl^- anions.[1c,d]

CHEMISTRY
AN ASIAN JOURNAL

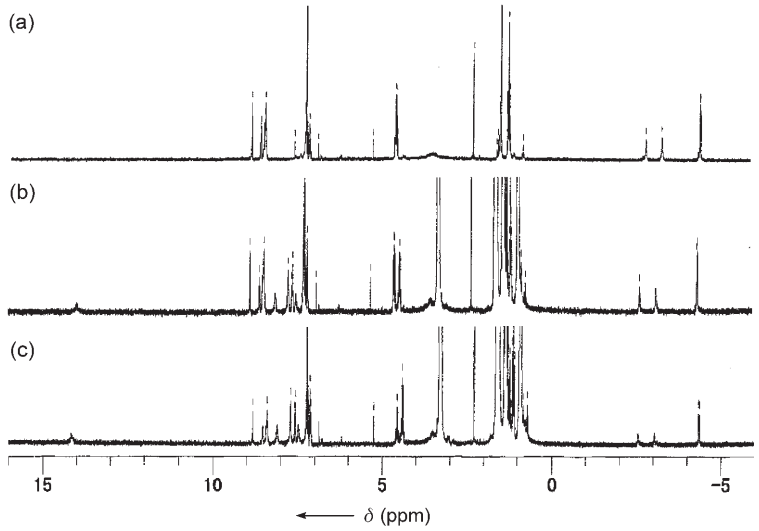

Figure 3. ^{1}H NMR spectra of **2** (2.2×10^{-3} M) in the presence of tetrabutylammonium chloride: a) 0 equiv, b) 1 equiv, and c) 2 equiv.

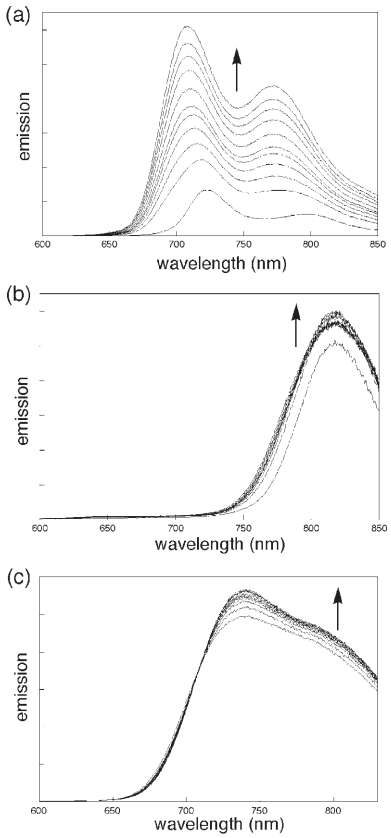

Figure 4. Changes in the fluorescence spectra of **1–3** upon the addition of tetrabutylammonium chloride in CH_2Cl_2. The excitation wavelength was fixed at one of the isosbestic points during titration: a) **1** (6.1×10^{-6} M, 442 nm), b) **2** (5.1×10^{-6} M, 479 nm), and c) **3** (6.8×10^{-6} M, 427 nm).

Anion Binding of NCP and N_2CP Metal Complexes

Although the anion binding of the free base NCP and N_2CPs is peculiar and attractive for anion sensing as described above, the associated NH tautomerism makes the binding mechanism somewhat complicated. To obtain clearer insight into the interactions between anions and NCPs, binding studies were performed on the metal complex systems in which the outer N–H atoms are fixed. Previously, the anion affinity of Ni^{II}–, Pd^{II}–, and Cu^{II}–NCP complexes (**1–M**) was reported briefly.[9] In this study, for comparison, Cu^{II} was chosen for the NCPs (**1–Cu**) as a divalent metal and Cu^{III} and Ag^{III} were utilized for N_2CPs (**2–Cu**, **3–Cu**, **3–Ag**) as trivalent metals (Scheme 3).[10–12] Again, the association constants for halide anions were determined from the changes in the absorption spectra upon titration. In contrast to the free bases, the intensity of the Soret bands increased, whereas that of the Q-like bands decreased. For example, in the case of **2–Cu**, the band at 451.5 nm increased and the band at 784.0 nm decreased with isosbestic points at 421, 729, and 763 nm upon the addition of Cl^- (Figure 5a). These spectral changes were totally different

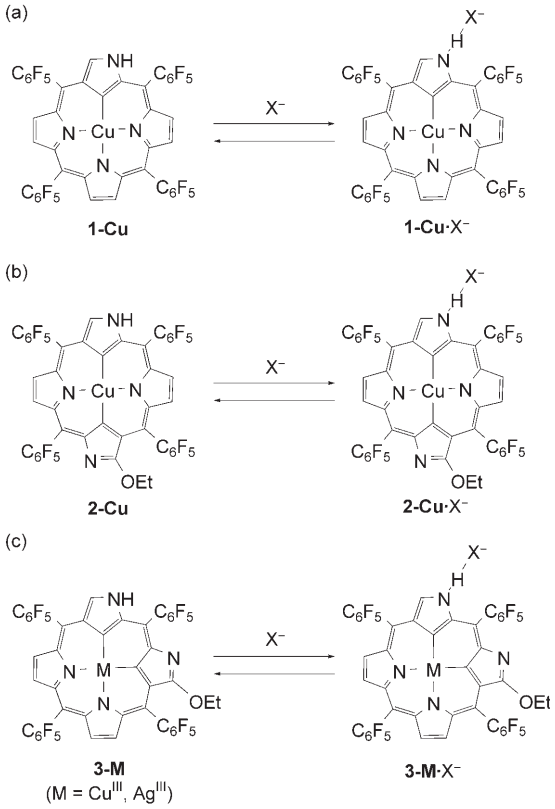

Scheme 3. Schematic representations of anion binding of a) **1–Cu**, b) **2–Cu**, and c) **3–M**.

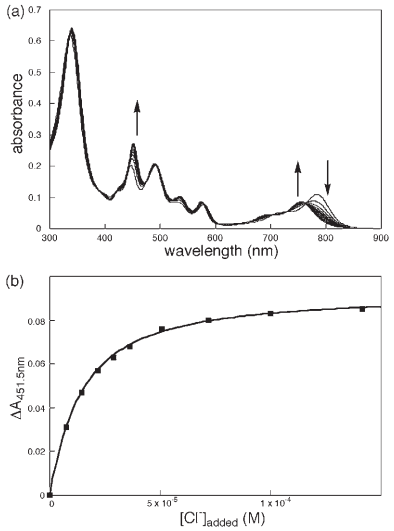

Figure 5. a) Changes in the absorption spectra of **2–Cu** (6.1×10^{-6} M) upon the addition of tetrabutylammonium chloride and b) titration plots fitting to 1:1 saturation curve.

from those of the deprotonated species, which show shifted Soret and weakened Q bands, probably as the result of a large perturbation of the π-ring system of the porphyrin core.[12b] The analysis of the binding curve afforded an association constant $K_a=9.0\times10^4\,M^{-1}$, which was about twofold larger than that of **1–Cu** (Figure 5b). A similar tendency was also observed with Br^- and I^- binding (Table 2). In contrast, a much smaller affinity was found with the *cis* isomer (**3–M**). For example, the K_a value of **3–Cu** for Cl^- was $9.2\times10^3\,M^{-1}$, which was about 1/5 and 1/10 of **1–Cu** and **2–Cu**, respectively, and the affinity order for the anions $Cl^->Br^->I^-$ was the same as that of free bases. In addition, the similar K_a values of **3–Cu** and **3–Ag** may suggest that the anion binding in the above NCP systems is not largely affected by the central metal species as long as an identical metal oxidation state is involved.

Table 2. Association constants (M^{-1}) of **1–Cu**, **2–Cu**, **3–Cu**, and **3–Ag** for halide anions as tetrabutylammonium salts in CH_2Cl_2.

Anions	**1–Cu**[a]	**2–Cu**	**3–Cu**	**3–Ag**
Cl^-	4.9×10^4	9.0×10^4	9.2×10^3	7.4×10^3
Br^-	6.9×10^3	2.7×10^4	1.6×10^3	1.7×10^3
I^-	1.2×10^3	1.9×10^3	210	90

[a] From reference [9].

Similar to the free-base systems, anion binding at the peripheral NH moiety of **2–Cu** and **3–M** was suggested by the changes in the ^{1}H NMR spectra upon the addition of Cl^- (Figure 6 and Supporting Information). For example, the signal for the peripheral NH proton of **2–Cu** (1.1×10^{-3} M) shifted downfield from $\delta=10.24$ to 14.96 ppm upon the addition of 1 equivalent of Cl^-. The corresponding chemical shifts of **3–Cu** and **3–Ag** ($\approx2\times10^{-3}$ M each) in the presence of 1 equivalent of Cl^- (and those of the anion-free species)

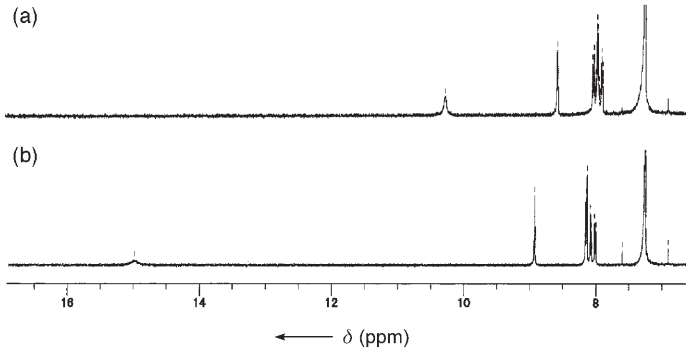

Figure 6. ^{1}H NMR chemical shifts of **2–Cu** (1.1×10^{-3} M): a) without Cl^- and b) with 1 equivalent of Cl^- as a tetrabutylammonium salt in $CDCl_3$.

were $\Delta\delta=14.85$ (10.30) and 14.64 (10.08) ppm, respectively. Consistent with the suggested 1:1 binding mode, the chemical-shift changes were saturated when almost 1 equivalent of Cl^- had been added.[9b]

Previously, we reported changes in the ^{19}F NMR signals of the diamagnetic Ni^{II} complex (**1–Ni**, 2×10^{-3} M) upon the addition of Cl^- as a tetrabutylammonium salt in $CDCl_3$:[9b] In the presence of 1 equivalent of Cl^-, the ^{19}F NMR signals of the C_6F_5 group neighboring the peripheral NH proton shifted upfield ($\Delta\delta=-1.4$ to -2.6 ppm), whereas the remaining signals for C_6F_5 were almost unchanged. Similar shifts were also observed with **2–Cu** and **3–M**; for *ortho*-, *para*-, and *meta*-F atoms: **2–Cu**: $\delta=-137.10$ ppm ($\Delta\delta=-1.42$ ppm), $\delta=-152.35$ ppm ($\Delta\delta=-2.64$ ppm), $\delta=-161.08$ ppm ($\Delta\delta=-1.70$ ppm); **3–Cu**: $\delta=-136.81$ ppm ($\Delta\delta=-0.79$ ppm), $\delta=-154.26$ ppm ($\Delta\delta=-3.26$ ppm), $\delta=-162.51$ ppm ($\Delta\delta=-1.93$ ppm) (Figure 7); **3–Ag**: $\delta=-136.83$ ppm ($\Delta\delta=-0.71$ ppm), $\delta=-154.18$ ppm ($\Delta\delta=-3.07$ ppm), $\delta=-162.42$ ppm ($\Delta\delta=-1.78$ ppm), respectively. The changes in the chemical shifts of the ^{19}F NMR signals are comparable in all the anion-bound metal complexes, indicating the same shielding effect by the negative charge of anions associated at the peripheral NH. Furthermore, when the outer *N*-methyl NCP–Cu^{II} complex was subjected to a similar titra-

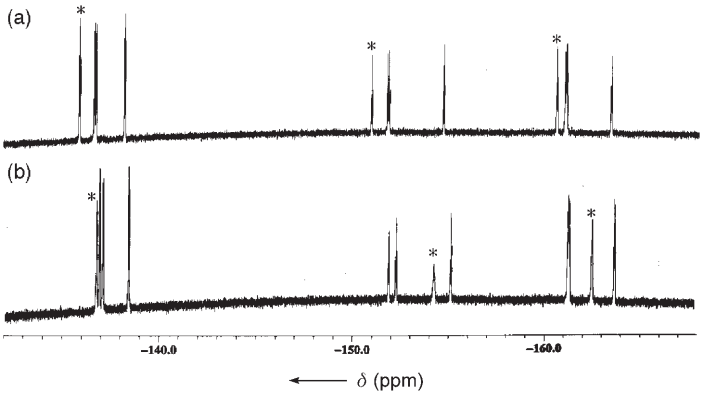

Figure 7. ^{19}F NMR chemical shifts of **3–Cu** (2×10^{-3} M): a) without Cl^- and b) with 1 equivalent of Cl^-. The signals for the C_6F_5 groups nearest the peripheral NH are marked with an asterisk (*).

tion, no changes were observed in either the UV/Vis or the ESR spectra, which excludes the possibility of axial coordination of Cl^- at the central metal atom.[9] These results strongly support halide binding at the peripheral NH moiety in solution.

Driving Force of Anion Binding of N-Confused Porphyrins

Normally, anion binding of a simple pyrrole through one-point hydrogen bonding is considered relatively weak. In fact, a small association constant, $K_a = 9.2\,M^{-1}$, was reported with 2,5-dimethylpyrrole for F^- binding in CD_2Cl_2,[4a] and we also obtained a small K_a value, $10\,M^{-1}$, with unsubstituted pyrrole for Cl^- binding in CD_2Cl_2. Thus, the estimated association constants for halide anions of NCPs seem abnormally large. Why can NCP and N_2CP bind anions so efficiently? What are the main factors that control their anion binding? To obtain clues regarding questions on the effective anion binding and the differences in anion affinity among NCPs, we examined the following factors: 1) zwitterionic resonance, 2) ion–dipole interactions, 3) polarizability, and 4) anion–π interactions.

Zwitterionic Resonance

As mentioned previously, the free base NCP and N_2CP exhibit several tautomeric forms that differ in aromaticity, and the metal complexes in this study maintain the framework of less-aromatic tautomers. In spite of the disconnection of full conjugation pathways at the confused pyrrole rings in the constitutional formula, both the free bases and the metal complexes exhibit the aromatic properties. This could be explained simply by assuming the zwitterionic resonance forms that contain the aromatic circuits (Scheme 4).[23]

In the resonance structures, the outer NH groups in all three NCPs carry partial positive charges. Thus, if such charge localization takes place, the NH groups would be highly polarized, and as a consequence the local charge–charge interactions between the outer NH and Cl^- is expected to be significant. To clarify the polarization, the charge density of the outer NH groups of the Cu complexes was evaluated by DFT calculations by means of the B3LYP method.[24] The natural population analysis (NPA)[25] charges on the outer NH atoms in each ligand (**1–Cu**, **2–Cu**, **3–Cu**) at the 6-31+G(d,p)//6-31G(d,p) basis-set level are around +0.45 (H) and −0.53 (N), which are much larger than those of the peripheral β-CH atoms of the normal pyrrole groups in the core (≈+0.25 (H) and −0.22 to −0.30 (C)), and almost similar to those of unsubstituted pyrrole, +0.445 (H) and −0.571 (N) (Table 3). These calculations indicate that the outer NH groups of the confused pyrroles are polarized as in the case of unsubstituted pyrrole, but the large distribution of partial positive charge on the outer NH groups inferred from the zwitterionic resonance forms is not so obvious.

When the NPA charges on the pyrrole rings of each complex were added and the values were compared with those of corresponding pyrroles in skeletons (**1*–Cu**, **2*–Cu**, **3*–Cu**), shifts of partial negative charge from the porphyrin cores to the electron-withdrawing *meso*-C_6F_5 groups were clearly observed, as expected (Table 3). For example, charge of approximately −0.15 e was transferred from the confused

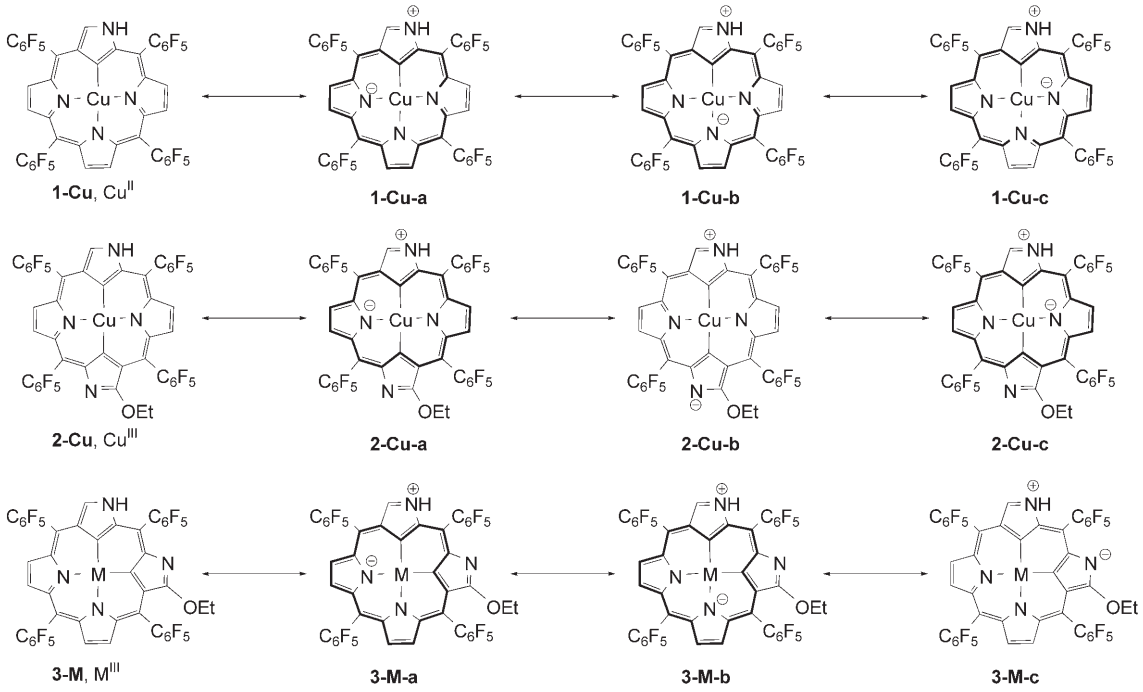

Scheme 4. Neutral (left) and zwitterionic resonance forms (**a**, **b**, **c**) of divalent metal complexes of NCP complex (**1–Cu**) and trivalent *trans*- and *cis*-N_2CP (**2–Cu**, **3–M**). 18π aromatic circuits are indicated in bold.

Table 3. The NPA charge of the outer NH atoms and of the pyrrole rings of **1–Cu**, **2–Cu**, **3–Cu**, NCTPP–Cu, their skeletons **1*–Cu**, **2*–Cu**, **3*–Cu**, and pyrrole at the B3LYP/6-31+G(d,p)//6-31G(d,p) level.

Compound	NPA charge		Sum of NPA charge on pyrrole ring[a,b]			
	Outer N	Outer H	Pyrrole-1	Pyrrole-2	Pyrrole-3	Pyrrole-4
1–Cu	−0.538	0.452	−0.193	−0.143	−0.193	−0.208
			(+0.150)	(+0.220)	(+0.071)	(+0.137)
2–Cu	−0.532	0.453	−0.167	−0.198	−0.188[c]	−0.157
			(+0.146)	(+0.123)	(+0.176)	(+0.133)
3–Cu	–0.520	0.456	−0.069	−0.201[c]	−0.130	−0.218
			(+0.142)	(+0.021)	(+0.221)	(+0.132)
NCTPP–Cu	−0.544	0.456	−0.234	–0.210	–0.250	–0.276
			(+0.109)	(+0.153)[c]	(+0.014)	(+0.069)
1*–Cu	−0.541	0.447	−0.343	−0.363	−0.264	−0.345
2*–Cu	−0.537	0.450	−0.313	−0.321	−0.364[c]	−0.290
3*–Cu	−0.525	0.451	−0.211	−0.222[c]	−0.351	−0.350
pyrrole	−0.571	0.445	–	–	–	–

[a] Pyrrole rings 1–4 are labeled clockwise from the NH-containing confused pyrrole (top) in the structures of Scheme 4. [b] Differences in the NPA charge between C_6F_5 and C_6H_5 derivatives and skeletons are shown in parentheses. [c] Calculated on C4N atoms in ethoxy-substituted pyrroles.

pyrroles (pyrrole-1) through the inductive effects of C_6F_5 groups in all three complexes. Such a large decrease in the negative charge from the porphyrin rings, especially from the confused pyrrole rings, may be important to strengthen the interactions with anions. Interestingly, when C_6F_5 groups were replaced by C_6H_5 groups, the amount of charge transfer became much smaller and was around −0.11 e, which suggests a weaker anion binding of phenyl-substituted NCPs.[26] In fact, this may rationalize the previous observation that the Ni^{II} complex of N-confused tetraphenylporphyrin (NCTPP–Ni) showed a small K_a value ($<10\,M^{-1}$) for Cl^-, whereas C_6F_5-substituted **1–Ni** leads to a large K_a value, $5.7\times10^4\,M^{-1}$, similar to that of **1–Cu**.[9b,27]

To check the reliability of the calculations on the present anion-binding systems, we evaluated the relative stability of each anion complex (and that of the skeletons **1*–Cu**, **2*–Cu**, **3*–Cu**) at the B3LYP/6-31+G(d,p)//6-31G(d,p) level. The stability energy (ΔE) of each anion complex was calculated by subtracting the sum of the total energy of free ligand (E_{free}) and Cl^- (E_{Cl}) from the total energy of the anion complex ($E_{complex}$) [Eq. (1)].[28]

$$\Delta E = E_{complex} - (E_{free} + E_{Cl}) \quad (1)$$

The results are summarized in Table 4. Consistent with the binding experiments, the ΔE values of the three complexes decrease in the same order as that of the K_a values, i.e., **2–Cu–Cl** > **1–Cu–Cl** > **3–Cu–Cl** (and **2*–Cu–Cl** > **1*–Cu–Cl** > **3*–Cu–Cl**). In the optimized structures of anion complexes, the distances between the anion and hydrogen-bonding N atom (N–H···Cl^-) are 2.94, 2.93, and 2.92 Å, and the corresponding bond angles (∢N-H···Cl^-) are 166.1, 165.6, and 165.8°, for **1–Cu–Cl**, **2–Cu–Cl**, and **3–Cu–Cl**, respectively (Figure 8). Both the hydrogen-bond length and angle in each complex are much smaller than those of the Cl^- complexes of the unsubstituted pyrrole (3.13 Å, 180°) and the skeletons (2.96 Å, 176°). The shorter bond lengths may reflect the tight anion binding of NCPs, and the bent angles could be attributed to the steric or electronic repulsion of a C_6F_5 group nearby (see below).

Ion–Dipole Interactions

The tenfold difference between the K_a values of **2–Cu** and **3–Cu** is of particular interest. What is the main factor in differentiating the anion-binding affinity between *trans*- and *cis*-N_2CP? In this study, we paid attention to the ion–dipole interactions between the NCPs and the anions, because the dipole moment (μ) could change substantially on the basis of the molecular structure. Theoretically, the potential energy of ion–dipole interactions is given by Equation (2) (ε_0 = permittivity of the vacuum, Ze = charge on the ion, r =

Table 4. The calculated total energy of anion complex ($E_{complex}$), free ligand (E_{free}), interaction energy (ΔE), energy of ion–dipole interaction ($E_{ion-dipole}$) and ion–induced dipole interaction ($E_{ion-induced\ dipole}$), and hydrogen-bond length and angle between anion and peripheral nitrogen atom (R and Φ) of various anion complexes.

Anion complex	$E_{complex}$ [Hartree]	E_{free} [Hartree]	ΔE[a] [kcal mol^{-1}]	$E_{ion-dipole}$ [kcal mol^{-1}]	$E_{ion-induced\ dipole}$ [kcal mol^{-1}]	$R_{NH\cdots Cl^-}$ [Å]	$\Phi_{NH\cdots Cl^-}$ [deg]
1–Cu–Cl	−5998.024946	−5537.681124	−43.36	−6.17	−8.76	2.94	166.1
2–Cu–Cl	−6151.224168	−5690.876718	−45.64	−7.21	−8.31	2.93	165.6
3–Cu–Cl	−6151.241386	−5690.898495	−42.77	−4.64	−8.82	2.92	165.8
1*–Cu–Cl	−3089.104816	−2628.779349	−31.84	−5.97	−5.22	2.97	175.9
2*–Cu–Cl	−3242.300648	−2781.972386	−33.59	−7.02	−4.18	2.96	175.9
3*–Cu–Cl	−3242.319207	−2781.994954	−31.08	−4.54	−5.20	2.96	175.6
pyrrole-Cl	−670.493340	−210.188153	−19.11	−7.45	−4.53	3.13	180.0

[a] $\Delta E = E_{complex} - (E_{free} + E_{Cl})$, $E_{Cl} = -460.274726$ Hartree. Calculations were performed at the B3LYP/6-31+G(d,p)//6-31G(d,p) level.

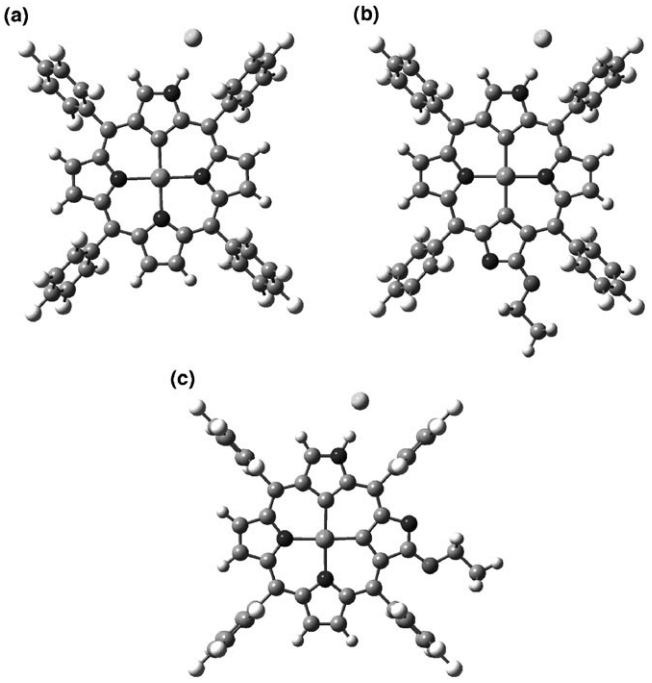

Figure 8. Optimized structures of anion complexes a) **1–Cu–Cl**, b) **2–Cu–Cl**, and c) **3–Cu–Cl**.

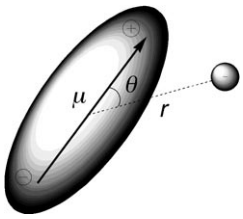

Figure 9. Schematic drawing of ion–dipole interactions. The direction of the dipole moment corresponds to the direction from the negative to the positive charge.

distance from the ion to the center of the dipole, θ = dipole angle relative to the line r joining the ion and the center of the dipole; Figure 9).[15]

$$E_{\text{ion-dipole}} = -\frac{Ze}{4\pi\varepsilon_0}\frac{\mu\cos\theta}{r^2} \qquad (2)$$

The dipole moments of NCPs are calculated for the optimized structures obtained from both anion-free systems and anion complexes. As expected, the magnitude and orientation of dipole moments change substantially and reflect the molecular structures (Figure 10). Very interestingly, the magnitudes follow the same order as the K_a values, that is, **2–Cu** > **1–Cu** > **3–Cu**, and the molecular dipoles of **1–Cu** and **2–Cu** point toward the outer NH groups, but that of **3–Cu** is slightly away from the outer NH group (Figure 10).

The estimated energies of the ion–dipole interactions in the anion complexes **1–Cu–Cl**, **2–Cu–Cl**, and **3–Cu–Cl** as well as their skeletons are summarized in Table 4. For the calculations, dipole moments derived from the anion complexes were utilized. The difference in the interaction energies between **2–Cu–Cl** and **3–Cu–Cl** is significantly large, 2.57 kcal mol^{-1}, and the energies decrease in the same order as the K_a values, that is, **2–Cu** > **1–Cu** > **3–Cu**. These results may suggest that the ion–dipole interaction is an important factor in the differentiation of the anion affinity of NCPs. At this point it is worth mentioning that the above ion–dipole interaction is characteristic of NCPs because 1) NCPs exhibit intrinsic large dipole moments reflecting the unsymmetrical structures owing to the confusion, and 2) the binding at the periphery enables an attraction of the anions closer to the molecular plane which is advantageous in gaining a large interaction energy (Equation (2)). In the case of ordinary porphyrins, on the other hand, the dipole moments are usually small owing to the symmetrical structure, and additional substituents are required to introduce anion-binding sites around the molecules.

Polarizability

Next, the interaction between an anion and induced dipole was estimated. The polarization of neutral NCP species depend on their inherent polarizability α and on the polarizing field E of the neighboring ion.[15] The interaction energies estimated from Equation (3) are shown in Table 4. The energies are around 9 kcal mol^{-1}, which are much larger than the ion–dipole interaction, but the difference among the NCPs was small (< 1 kcal mol^{-1}). Interestingly, the corresponding energies for skeletons are about 4 kcal mol^{-1} smaller than those for C_6F_5-substituted species. These results indicate that the ion–induced dipole interaction contributes largely to enhance the anion affinity.

$$E_{\text{ion-induceddipole}} = -\frac{1}{2}(\alpha E)\cdot E \qquad (3)$$

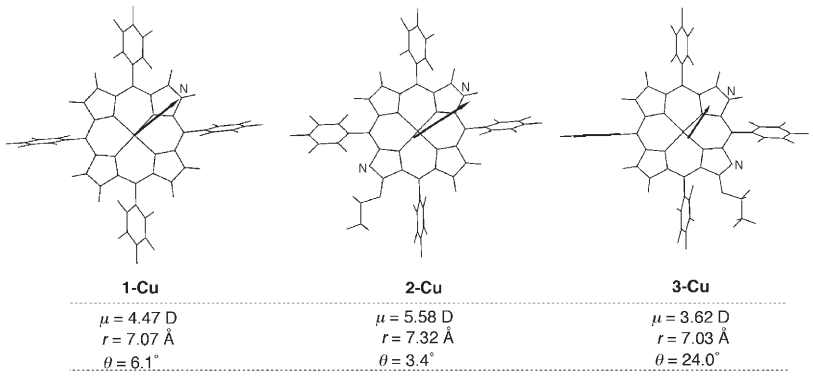

Figure 10. Schematic drawings of dipole moments of N-confused porphyrins (anion-free) and geometry of anion–dipole interactions.

Anion–π Interaction

Noncovalent electrostatic bonding between anions and electron-deficient aromatic rings (anion–π interaction) is a current hot topic.[14] In the system under study, the halide anions bound to the outer NH moiety are located near the C_6F_5 group at the *meso*-position of NCPs. Such a close arrangement of an anion and an electron-deficient aromatic ring make this binding system attractive from a point of view of anion–π interactions (Figure 11). If the anion–π interactions are significant, even in the solution, then incorporation of an electron-deficient group near the anion-binding site would become a general method in designing anion receptors.

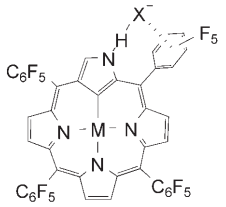

Figure 11. Schematic drawing of hypothetical anion–π interaction.

To clarify whether anion–π interactions are actually at play in the NCP systems, we synthesized a series of tri-C_6F_5-substituted NCP–Ni^{II} complexes (**4–Ni**, **5–Ni**, **6–Ni**) to examine the Cl^--binding affinity (Figures 12 and 13).[29] **7–Ni** was not yet synthesized. The initial idea was that if the magnitude of the anion–π interactions is relatively large, a somewhat smaller K_a value would be obtained with **4–Ni** because it lacks a C_6F_5 group nearby. UV/Vis titration experiments with Cl^- in CH_2Cl_2 gave K_a values of 4.4×10^4, 4.2×10^4, and $2.6\times10^4\,M^{-1}$ for **4–Ni**, **5–Ni**, and **6–Ni**, respectively. These values are smaller than that of tetra-C_6F_5-substituted **1–Ni** ($5.7\times10^4\,M^{-1}$), and this weaker affinity of trisubstituted NCPs could be attributed to the polarization change owing to the decreased number of electron-withdrawing C_6F_5 groups at the *meso* positions. Furthermore, in contrast to the planar tetrasubstituted NCP complex **1–Ni**,[10] the optimized structures of trisubstituted complexes are largely distorted, and thus the molecules are likely to be fluttering in solution to destabilize the anion–π complex, resulting in the lower anion affinity of **6–Ni**. In spite of the absence of a C_6F_5 group at the *meso* position close to the outer NH, the anion-binding affinity of **4–Ni** is nearly same as that of **5–Ni** and larger than that of **6–Ni** (**4–Ni** ≈ **5–Ni** > **6–Ni**), suggesting the anion–π interactions are not large, if they are at all present; rather, they are repulsive. In this case again, the ion–dipole and ion–induced dipole interactions are significant, and both interaction energies vary substantially according to the position of the *meso* C_6F_5 groups (Table 5). In contrast to the tetrasubstituted NCP, a detail analysis of the present trisubstituted NCP system is complicated because the partial negative-charge shifts from the confused pyrrole rings differ largely according to the position of the C_6F_5 groups (Supporting Information, Table S3) Furthermore, the solvation issue needs to be taken into account seriously. For complexes lacking a *meso*-aryl group near the anion-binding site (**4–Ni** or **6–Ni**), anion complexation might be largely disturbed by attack of the solvent molecules, whereas in the case of **5–Ni** or **7–Ni** such interactions might be suppressed to some degree by the *meso*-aryl groups, which serve as a protective wall around the anion-binding site. Hence, important points to be considered in the development of efficient anion receptors based on NCP skeletons are the rigidity of the molecule, which suppresses the fluttering motion, and electron-withdrawing *meso* aryl groups, which enhance the polarization and serve as a barrier against solvent attack.

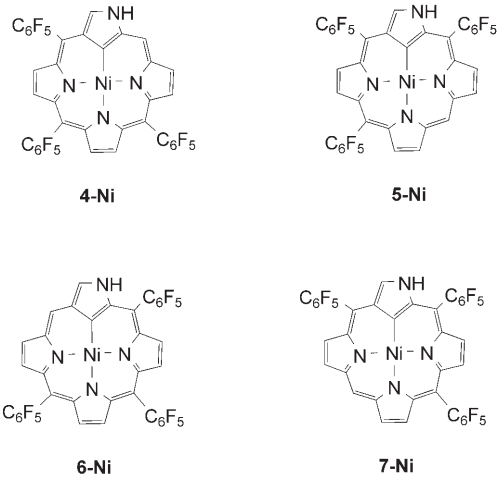

Figure 12. Ni^{II} complexes of trisubstituted N-confused porphyrins.

Ion-Pair Complex

Attempts to obtain single crystals of anion-bound NCP complexes have not been successful so far. However, a different type of crystal in which an NCP anion and a tetrabutylam-

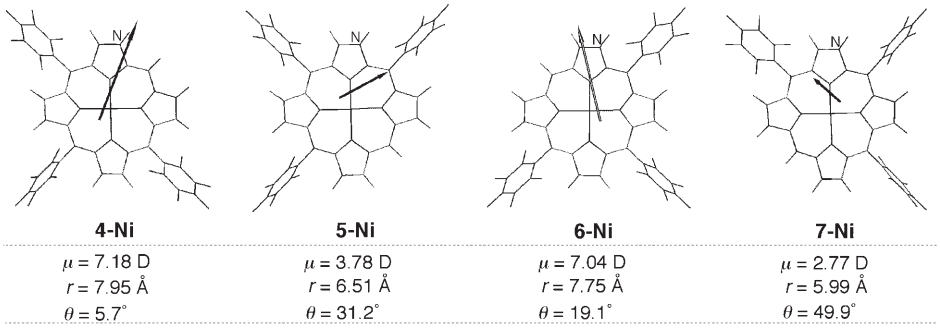

Figure 13. Schematic drawings of dipole moments of Ni^{II} complexes of trisubstituted NCPs (anion-free) and geometry of anion–dipole interactions.

Table 5. The calculated total energy of anion complex ($E_{complex}$), free ligand (E_{free}), interaction energies (ΔE), energy of ion–dipole interaction ($E_{ion-dipole}$) and ion–induced dipole interaction ($E_{ion-induced\ dipole}$), and hydrogen-bond length and angle between anion and nitrogen atom (R and Φ) of trisubstituted NCP anion complexes.

Anion complex	$E_{complex}$ [Hartree]	E_{free} [Hartree]	ΔE [kcal mol^{-1}]	$E_{ion-dipole}$ [kcal mol^{-1}]	$E_{ion-induced\ dipole}$ [kcal mol^{-1}]	$R_{NH\cdots Cl^-}$ [Å]	$\Phi_{NH\cdots Cl^-}$ [°]
4–Ni–Cl	−5138.676100	−4678.336205	−40.89	−7.85	−4.32	2.94	172.6
5–Ni–Cl	−5138.677500	−4678.337372	−41.04	−5.29	−11.38	2.94	165.9
6–Ni–Cl	−5138.677126	−4678.335927	−41.71	−7.68	−5.36	2.94	165.7
7–Ni–Cl	−5138.677365	−4678.337349	−40.97	−3.45	−14.39	2.94	165.7

monium cation (nBu$_4$N$^+$) form an ion-pair complex was obtained from a solution mixture of **1–Cu** and nBu$_4$NCl (Figure 14, Table 6).[30] In the crystal, the nBu$_4$N$^+$ is located

Table 6. Summary of crystallographic data for **1–Cu$^-$·N(C$_4$H$_9$)$_4^+$**

	1–Cu$^-$·N(C$_4$H$_9$)$_4^+$
formula	$C_{56}H_{43}N_5CuF_{20}$
FW	1229.49
crystal size [mm^3]	0.20 × 0.11 × 0.08
crystal system	tetragonal
space group	*I*4*m* (no. 87)
a [Å]	18.0761(18)
b [Å]	18.0761(18)
c [Å]	8.2550(11)
α [°]	90
β [°]	90
γ [°]	90
V [Å^3]	2697.3(5)
ρ_{calcd} [g cm^{-3}]	1.513
Z	2
T [K]	273
no. of reflections	1331
no. of unique reflections	1072
variables	131
$\lambda_{MoK\alpha}$ [Å]	0.71073
R_1 [$I > 2\,\sigma(I)$]	0.0547
wR_2 [$I > 2\,\sigma(I)$]	0.1611
goodness of fit	1.068

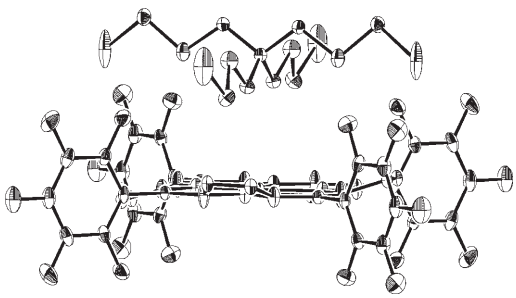

Figure 14. Crystal structure of an ion-pair complex of a **1–Cu** anion and a tetrabutylammonium cation. Hydrogen atoms are omitted for clarity.

4.13 Å above or below the NCP anion plane and two molecules stack each other, forming one-dimensional columns (Supporting Information Figure S9). Interestingly, Cl$^-$ anions are not included in the crystal. Presumably, the Cl$^-$ anion in the neutral-pair complex served as a base to dissociate the outer NH hydrogen of NCPs, affording a volatile HCl and an ion-pair complex of NCP$^-$ and nBu$_4$N$^+$ during the preparation of single crystals.[31] This result may also reflect the highly polarized nature of the confused pyrrole ring of the C$_6$F$_5$-substituted NCPs.

Summary

NCP (**1**) and *trans*- (**2**) and *cis*-N$_2$CPs (**3**) bind halide anions Cl$^-$, Br$^-$, I$^-$ efficiently in CH$_2$Cl$_2$ at the peripheral NH moieties. For the free bases, anion-induced NH tautomerism was observed and *cis*-N$_2$CP **3** showed the highest affinity for Cl$^-$ and Br$^-$, whereas, among the metal complexes, *trans*-N$_2$CP **2–Cu** exhibited the highest affinity to all halide anions. The larger affinity of NCPs and N$_2$CPs for halide anions was attributed to 1) hydrogen-bonding donor sites at the periphery, 2) inductive effects of the electron-withdrawing C$_6$F$_5$ groups, and 3) ion–induced dipole and ion–dipole interactions between the NCP molecules and the anions, where the former is characteristic of the large π systems of porphyrins with aryl groups at the *meso* positions and the latter change largely according to the number and position of the confused pyrrole rings. Anion–π interactions are not likely to be involved in the present anion-binding systems.

The anion binding described herein may not only disclose the intrinsic nature of NCPs, but may also offer a general strategy for designing novel anion receptors: Large π systems that exhibit high polarizability, a large dipole moment with an appropriate orientation, and an anion trap through hydrogen bonding, or a combination of these factors, may serve as the basis for synthetic anion receptors.

Experimental Section

General Procedures

Commercially available solvents and reagents were used without further purification unless otherwise mentioned. Silica-gel column chromatography was performed on Wakogel C-200 and C-300. Thin-layer chromatography (TLC) was carried out on aluminum sheets coated with silica gel 60 (Merck 5554). UV/Vis spectra were recorded on a Shimadzu UV-3150PC spectrometer. Fluorescence emission spectra were recorded on a Horiba Fluorolog-3 spectrometer. ^{1}H NMR spectra were recorded on a JEOL JNM-AL300 spectrometer (operating at 300.00 MHz for ^{1}H NMR, residual solvent was used as internal reference). ^{19}F NMR spectra were recorded on a JEOL ECA600 spectrometer (operating at 564.73 MHz, C$_6$F$_6$ used as the external reference). Fast atom bombardment mass spectra (FAB MS) were recorded on a JEOL-HX110 in the positive-ion mode with a 3-nitrobenzyl alcohol matrix. Preparation of **1–3** and the metal complexes was reported previously.[10–12]

N-confused 1-formyl-9-pentafluorobenzoyldipyrromethane: Formylation of N-confused 9-pentafluorobenzoyldipyrromethane was carried out with CH_3OCHCl_2 and $AlCl_3$ according to a previously reported method.[32] Yield: 52%. ^{1}H NMR (300 MHz, $CDCl_3$): δ=9.53 (s, 1H; CHO), 9.50 (br, 1H; NH), 9.42 (br, 1H; NH), 7.08 (s, 1H; pyrrole-H), 6.93 (s, 1H; pyrrole-H), 6.66 (s, 1H; pyrrole-H), 6.13 (m, 1H; pyrrole-H), 5.83 ppm (s, 1H; *meso*-H); MS (FAB): *m/z* (%) calcd for $C_{23}H_8F_{10}N_2O_2$: 534.04 $[M]^+$; found: 534.3 (60) $[M]^+$, 535.3 (100) $[M+1]^+$.

4: $NaBH_4$ (358 mg, 10.0 mmol) was added to a solution of N-confused 1-formyl-9-pentafluorobenzoyldipyrromethane (100 mg, 0.188 mmol) in THF/MeOH (4:1 *v/v*; 12 mL), and the solution was stirred at room temperature for 1 day. After checking the disappearance of starting material by TLC, the reaction mixture was poured into CH_2Cl_2. The organic layer was separated, washed with water and brine, and dried over anhydrous Na_2SO_4. After evaporation, the dicarbinol was obtained as a yellow oil, and the crude product was used for the next reaction without further purification. The dicarbinol ($\approx$0.188 mmol) was dissolved in a solution of 5-pentafluorophenyldipyrromethane (58.7 mg, 0.188 mmol) in CH_2Cl_2 (190 mL), and methanesulfonic acid (4 μL) was added. After stirring at room temperature for 1 h, the reaction mixture was passed through a silica-gel column (Wakogel C-200) and eluted with CH_2Cl_2. DDQ (63 mg, 0.28 mmol) was added to the solution, which was stirred for 15 min at room temperature. Separation by silica-gel column chromatography (Wakogel C-300, CH_2Cl_2) afforded the purple product **4** (1.6% yield). UV/Vis (CH_2Cl_2): λ_{max}=429, 524, 564, 699 nm; ^{1}H NMR (300 MHz, $CDCl_3$): δ=10.35 (s, 1H; *meso*-CH), 9.39 (d, J=4.8 Hz, 1H; βCH), 9.06 (s, 1H; αCH), 8.91 (d, J=4.8 Hz, 1H; βCH), 8.73 (d, J=4.8 Hz, 1H; βCH), 8.67 (d, J=4.8 Hz, 1H; βCH), 8.65 (d, J=4.8 Hz, 1H; βCH), 8.59 (d, J=4.8 Hz, 1H; βCH), −2.54 (br, 1H; inner NH), −2.93 (br, 1H; inner NH), −5.42 ppm (s, 1H; inner CH); MS (FAB): *m/z* (%) calcd for $C_{38}H_{11}F_{15}N_4$: 808.07 $[M]^+$; found: 808.3 (25) $[M]^+$, 809.3 (100) $[M+1]^+$.

4–Ni: $Ni(acac)_2{\cdot}xH_2O$ (8 mg) was added to a solution of **4** (2.4 mg, 0.003 mmol) in $CHCl_3$ (10 mL), and stirred at reflux temperature for 15 h. Quantitative complexation was confirmed by TLC. After evaporation, the residue was passed through a silica-gel column (Wakogel C-300, CH_2Cl_2) to afford a reddish product. Recrystallization from CH_2Cl_2/hexane gave **4–Ni** as a purple solid (45% yield). UV/Vis (CH_2Cl_2): λ_{max} (ε)=340 (35000), 363 (36000), 416 (80000), 461 (23000), 557 (12000), 723 (2000), 797 nm ($2000\,M^{-1}\,cm^{-1}$); ^{1}H NMR (300 MHz, $CDCl_3$): δ=10.17 (br, 1H; outer-NH), 8.40 (s, 1H; *meso*-CH), 8.36 (br, 1H; αCH), 8.34 (d, J=5.1 Hz, 1H; βCH), 7.99 (d, J=5.7 Hz, 1H; βCH), 7.93 (d, J=5.7 Hz, 1H; βCH), 7.86 (d, J=5.1 Hz, 1H; βCH), 7.79 (d, J=4.8 Hz, 1H; βCH), 7.74 ppm (d, J=4.8 Hz, 1H; βCH); MS (FAB): *m/z* (%) calcd for $C_{38}H_9F_{15}N_4Ni$: 863.99 $[M]^+$; found: 864.3 (95) $[M]^+$, 865.3 (100) $[M+1]^+$.

5: $NaBH_4$ (1.39 g, 37.5 mmol) was added to a solution of bis(pentafluorobenzoyl) N-confused 5-pentafluorophenyldipyrromethane (530 mg, 0.75 mmol) in THF/MeOH (4:1 *v/v*; 50 mL), and the mixture was stirred at room temperature for 3 h. After the disappearance of starting material (TLC), the reaction mixture was poured into CH_2Cl_2, and the organic layer was separated, washed with water and brine, and dried over anhydrous Na_2SO_4. After evaporation, the dicarbinol was obtained as a yellow oil, and the crude product was used for the next reaction without further purification. The dicarbinol ($\approx$0.75 mmol) was dissolved in a solution of *meso*-free dipyrromethane (110 mg, 0.75 mmol) in CH_2Cl_2 (750 mL), and methanesulfonic acid (16 μL) was added. After stirring at room temperature for 1 h, the reaction mixture was passed through a silica-gel column (Wakogel C-200) and eluted with CH_2Cl_2. DDQ (255 mg, 1.13 mmol) was added, and the solution was stirred for 20 min at room temperature. Separation by silica-gel column chromatography (Wakogel C-300, CH_2Cl_2), followed by recrystallization from CH_2Cl_2/hexane gave **5** as a purple solid in 7.2% yield. UV/Vis (CH_2Cl_2): λ_{max}= 430, 525, 563, 640, 706 nm; ^{1}H NMR (300 MHz, $CDCl_3$): δ=9.95 (s, 1H; *meso*-CH), 9.21 (d, J=4.8 Hz, 1H; βCH), 9.13 (d, J=4.5 Hz, 1H; βCH), 8.99 (d, J=4.8 Hz, 1H; βCH), 8.91 (s, 1H; αCH), 8.87 (d, J=4.8 Hz, 1H; βCH), 8.68 (d, J=5.1 Hz, 1H; βCH), 8.63 (d, J=4.8 Hz, 1H; βCH), −2.61 (br, 1H; inner NH), −3.03 (br, 1H; inner NH), −5.54 ppm (s, 1H; inner CH); MS (FAB): *m/z* (%) calcd for $C_{38}H_{11}F_{15}N_4$: 808.07 $[M]^+$; found: 808.1 (45) $[M]^+$, 809.1 (100) $[M+1]^+$.

5–Ni: $Ni(acac)_2{\cdot}xH_2O$ (36.2 mg) was added to a solution of **5** (11.4 mg, 0.014 mmol) in $CHCl_3$ (40 mL), and the mixture was stirred at reflux temperature for 19 h. Quantitative complexation was confirmed by TLC. After evaporation, the residue was passed through a silica-gel column (Wakogel C-300, CH_2Cl_2) to afford a reddish product. Recrystallization from CH_2Cl_2/hexane gave **5–Ni** as a purple solid (33% yield). UV/Vis (CH_2Cl_2): λ_{max} (ε)=342 (31000), 417 (62000), 467 (17000), 561 (9000), 589 (8000), 734 (1700), 811 nm ($1900\,M^{-1}\,cm^{-1}$); ^{1}H NMR (300 MHz, $CDCl_3$): δ=10.01 (br, 1H; outer-NH), 8.64 (s, 1H; *meso*-CH), 8.42 (d, J=3.6 Hz, 1H; αCH), 8.35 (d, J=5.1 Hz, 1H; βCH), 8.23 (d, J=4.8 Hz, 1H; βCH), 7.98 (d, J=5.1 Hz, 1H; βCH), 7.93 (d, J=5.1 Hz, 1H; βCH), 7.87 (d, J=5.1 Hz, 1H; βCH), 7.70 ppm (d, J=5.4 Hz, 1H; βCH); MS (FAB): *m/z* (%) calcd for $C_{38}H_9F_{15}N_4Ni$: 863.99 $[M]^+$; found: 864.0 (100) $[M]^+$.

6: $NaBH_4$ (630 mg, 16.6 mmol) was added to a solution of bis(pentafluorobenzoyl) N-confused dipyrromethane (175 mg, 0.33 mmol) in THF/MeOH (4:1 *v/v*; 25 mL), and the solution was stirred at room temperature for 14 h. After the disappearance of starting material (TLC), the reaction mixture was poured into CH_2Cl_2, and the organic layer was separated, washed with water and brine, and dried over anhydrous Na_2SO_4. After evaporation, a dicarbinol was obtained as a yellow oil, and the crude product was used for the next reaction without further purification. The dicarbinol ($\approx$0.33 mmol) was dissolved in a solution of 5-pentafluorophenyl dipyrromethane (99.5 mg, 0.32 mmol) in CH_2Cl_2 (328 mL), and methanesulfonic acid (7.5 μL) was added. After stirring at room temperature for 1.5 h, the reaction mixture was passed through a silica-gel column (Wakogel C-200) and eluted with CH_2Cl_2. DDQ (201 mg, 0.885 mmol) was added to the combined solution, and stirred for 20 min at room temperature. The product was separated by silica-gel column chromatography (Wakogel C-300, CH_2Cl_2), and recrystallization from CH_2Cl_2/hexane gave **6** as a purple solid (2.3% yield). UV/Vis (CH_2Cl_2): λ_{max}=427, 522, 558, 635, 702 nm; ^{1}H NMR (300 MHz, $CDCl_3$): δ=10.10 (s, 1H; *meso*-CH), 9.57 (s, 1H; αCH), 9.37 (d, J=4.8 Hz, 1H; βCH), 8.99 (d, J=4.8 Hz, 1H; βCH), 8.73 (d, J=5.1 Hz, 1H; βCH), 8.68 (d, J=5.1 Hz, 1H; βCH), 8.64 (d, J=5.4 Hz, 1H; βCH), 8.62 (d, J=5.4 Hz, 1H; βCH), −2.67 (br, 1H; inner NH), −2.94 (br, 1H; inner NH), −5.46 ppm (s, 1H; inner CH); MS (MALDI-TOF): *m/z* (%) calcd for $C_{38}H_{11}F_{15}N_4$: 808.07 $[M]^+$; found: 808.5 (100) $[M]^+$.

6–Ni: $Ni(acac)_2{\cdot}xH_2O$ (16.4 mg) was added to a solution of **6** (5.0 mg, 0.0062 mmol) in $CHCl_3$ (15 mL) and stirred at reflux temperature for 15 h. Quantitative complexation was confirmed by TLC. After evaporation, the residue was passed through a silica-gel column (Wakogel C-300, CH_2Cl_2) to afford the reddish product. Recrystallization from CH_2Cl_2/hexane gave **6–Ni** as a purple solid (67% yield). UV/Vis (CH_2Cl_2): λ_{max} (ε)=343 (33000), 362 (32000), 415 (73000), 559 (12000), 714 (2300), 785 nm ($2000\,M^{-1}\,cm^{-1}$); ^{1}H NMR (300 MHz, $CDCl_3$): δ=10.04 (br, 1H; outer-NH), 8.98 (d, J=3.6 Hz, 1H; αCH), 8.93 (s, 1H; *meso*-CH), 8.39 (d, J=4.8 Hz, 1H; βCH), 7.98 (d, J=4.8 Hz, 1H; βCH), 7.91 (d, J=4.8 Hz, 1H; βCH), 7.89 (d, J=4.8 Hz, 1H; βCH), 7.78 (d, J=4.8 Hz, 1H; βCH), 7.74 ppm (d, J=4.8 Hz, 1H; βCH); MS (MALDI-TOF): *m/z* (%) calcd for $C_{38}H_9F_{15}N_4Ni$: 863.99 $[M]^+$; found: 864.4 (100) $[M]^+$.

DFT Calculations

DFT calculations of the basic frameworks of NCP (**1**), *trans*- (**2**), and *cis*-N_2CP (**3**) and their anion-binding complexes were carried out using the Gaussian 03 program[24] on IBM eServer p5 model 595 and PowerMac G5 computers. The structures were optimized at the B3LYP level by using a 6–31G(d,p) basis set, and the total electronic energies, dipole moment, and polarizability were calculated by using a 6–31+G(d,p) basis set.

Single-Crystal Diffraction Analysis

Data was collected on a Bruker SMART CCDC for **1–Cu·N(C_4H_9)$_4^+$**, refined by full-matrix least-squares procedures with anisotropic thermal parameters for the non-hydrogen atoms. Solutions of the structures were performed by using the *Crystal Structure* crystallographic software package (Molecular Structure Corporation). Crystals of **1–Cu·N(C_4H_9)$_4^+$** were obtained by vapor diffusion of hexane into a solution of **1–Cu** and

Bu_4NCl (1 equiv) in $CHCl_3$. Crystallographic details are summarized in Table 6. CCDC-284426 (**1–Cu·N(C_4H_9)$_4^+$**) contains the supplementary crystallographic data for this paper. These data can be obtained free of charge from the Cambridge Crystallographic Data Centre at www.ccdc.cam.ac.uk/data_request/cif.

Acknowledgements

The authors acknowledge Prof. Takuji Ogawa at the Institute for Molecular Science (Okazaki) for valuable discussions and Mr. Soji Shimizu at Kyoto University for help with ^{19}F NMR measurements. H.M. and T.M. thank JSPS for a Research Fellowship for Young Scientists. This work was partially supported by the Sumitomo Foundation and the Shorai Foundation.

[1] a) B. Dietrich, M. W. Hosseini, in *Supramolecular Chemistry of Anions* (Eds: A. Bianchi, K. Bowman-James, E. García-España), Wiley-VCH, New York, **1997**, pp. 45–62; b) M. W. Hosseini, A. J. Blacker, J.-M. Lehn, *J. Am. Chem. Soc.* **1990**, *112*, 3896–3904; c) P. D. Beer, *Acc. Chem. Res.* **1998**, *31*, 71–80; d) R. Martínez-Máñez, F. Sancenón, *Chem. Rev.* **2003**, *103*, 4419–4476.

[2] P. D. Beer, P. A. Gale, *Angew. Chem.* **2001**, *113*, 502–532; *Angew. Chem. Int. Ed.* **2001**, *40*, 486–516.

[3] a) C. H. Park, H. E. Simmons, *J. Am. Chem. Soc.* **1968**, *90*, 2431–2432; b) J.-M. Lehn, E. Sonveaux, A. K. Willard, *J. Am. Chem. Soc.* **1978**, *100*, 4914–4916; c) G. Müller, J. Riede, F. P. Schmidtchen, *Angew. Chem.* **1988**, *100*, 1574–1575; *Angew. Chem. Int. Ed. Engl.* **1988**, *27*, 1516–1518.

[4] a) P. A. Gale, J. L. Sessler, V. Král, V. Lynch, *J. Am. Chem. Soc.* **1996**, *118*, 5140–5141; b) P. A. Gale, J. L. Sessler, V. Král, *Chem. Commun.* **1998**, 1–8.

[5] a) J. L. Sessler, M. J. Cyr, V. Lynch, E. McGhee, J. A. Ibers, *J. Am. Chem. Soc.* **1990**, *112*, 2810–2813; b) M. Shionoya, H. Furuta, V. Lynch, A. Harriman, J. L. Sessler, *J. Am. Chem. Soc.* **1992**, *114*, 5714–5722; c) J. L. Sessler, J. Davis, *Acc. Chem. Res.* **2001**, *34*, 989–997.

[6] M. Huser, W. F. Morf, K. Fluri, K. Seiler, P. Schulthess, W. Simon, *Helv. Chim. Acta* **1990**, *73*, 1481–1496.

[7] a) H. Furuta, T. Asano, T. Ogawa, *J. Am. Chem. Soc.* **1994**, *116*, 767–768; b) P. J. Chmielewski, L. Latos-Grażyński, K. Rachlewicz, T. Głowiak, *Angew. Chem.* **1994**, *106*, 805–808; *Angew. Chem. Int. Ed. Engl.* **1994**, *33*, 779–781.

[8] a) L. Latos-Grażyński, in *The Porphyrin Handbook*, *Vol. 2* (Eds.: K. M. Kadish, K. M. Smith, R. Guilard), Academic Press, SanDiego, **2000**, chap. 14, pp. 361–416; b) H. Furuta, H. Maeda, A. Osuka, *Chem. Commun.* **2002**, 1795–1804; c) J. D. Harvey, C. J. Ziegler, *Coord. Chem. Rev.* **2003**, *247*, 1–19; d) H. Maeda, H. Furuta, *J. Porphyrins Phthalocyanines* **2004**, *8*, 67–75; e) A. Srinivasan, H. Furuta, *Acc. Chem. Res.* **2005**, *38*, 10–20; f) P. J. Chmielewski, L. Latos-Grażyński, *Coord. Chem. Rev.* **2005**, *249*, 2510–2533; g) M. Pawlicki, L. Latos-Grażyński, *Chem. Rec.* **2006**, *6*, 64–78; h) H. Maeda, H. Furuta, *Pure Appl. Chem.* **2006**, *78*, 29–44.

[9] a) H. Maeda, Y. Ishikawa, T. Matsuda, A. Osuka, H. Furuta, *J. Am. Chem. Soc.* **2003**, *125*, 11822–11823; b) H. Maeda, A. Osuka, H. Furuta, *J. Incl. Phenom.* **2004**, *49*, 33–36.

[10] H. Maeda, A. Osuka, Y. Ishikawa, I. Aritome, Y. Hisaeda, H. Furuta, *Org. Lett.* **2003**, *5*, 1293–1296.

[11] H. Maeda, A. Osuka, H. Furuta, *J. Am. Chem. Soc.* **2003**, *125*, 15690–15691.

[12] a) H. Furuta, H. Maeda, A. Osuka, *J. Am. Chem. Soc.* **2000**, *122*, 803–807; b) K. Araki, H. Winnischofer, H. E. Toma, H. Maeda, A. Osuka, H. Furuta, *Inorg. Chem.* **2001**, *40*, 2020–2025; c) K. Araki, F. N. Engelmann, I. Mayer, H. E. Toma, M. S. Baptista, H. Maeda, A. Osuka, H. Furuta, *Chem. Lett.* **2003**, *32*, 244–245; d) H. Maeda, A. Osuka, H. Furuta, *Supramol. Chem.* **2003**, *15*, 447–450; e) K. Araki, F. M. Engelmann, I. Mayer, H. E. Toma, M. S. Baptista, H. Maeda, A. Osuka, H. Furuta, *J. Photochem. Photobiol. A* **2004**, *163*, 403–411; f) H. Maeda, A. Osuka, H. Furuta, *Tetrahedron* **2004**, *60*, 2427–2432.

[13] S. Martinez-Carrera, *Acta Crystallogr.* **1966**, *20*, 783–788.

[14] a) H.-J. Schneider, *Angew. Chem.* **1991**, *103*, 1419–1439; *Angew. Chem. Int. Ed. Engl.* **1991**, *30*, 1417–1436; b) I. Alkorta, I. Rozas, J. Elguero, *J. Am. Chem. Soc.* **2002**, *124*, 8593–8598; c) D. Quiñonero, C. Garau, C. Rotger, A. Frontera, P. Ballester, A. Costa, P. M. Deyà, *Angew. Chem.* **2002**, *114*, 3539–3542; *Angew. Chem. Int. Ed.* **2002**, *41*, 3389–3392; d) D. Quiñonero, C. Garau, A. Frontera, P. Ballester, A. Costa, P. M. Deyà, *Chem. Phys. Lett.* **2002**, *359*, 486–492; e) M. Mascal, A. Armstrong, M. D. Bartberger, *J. Am. Chem. Soc.* **2002**, *124*, 6274–6276; f) C. Garau, D. Quiñonero, A. Frontera, P. Ballester, A. Costa, P. M. Deyà, *Org. Lett.* **2003**, *5*, 2227–2229; g) S. Demeshko, S. Dechert, F. Meyer, *J. Am. Chem. Soc.* **2004**, *126*, 4508–4509; h) C. Garau, A. Frontera, P. Ballester, D. Quiñonero, A. Costa, P. M. Deyà, *Eur. J. Org. Chem.* **2005**, 179–183.

[15] a) C. Reichardt, *Solvents and Solvents Effects in Organic Chemistry*, Wiley-VCH, Weinheim, **2003**, pp. 10–14; b) J. N. Israelachvili, *Intermolecular and Surface Forces*, Academic Press, London, **1992**.

[16] H. Furuta, T. Ishizuka, A. Osuka, H. Dejima, K. Nakagawa, Y. Ishikawa, *J. Am. Chem. Soc.* **2001**, *123*, 6207–6208.

[17] H. Furuta, H. Maeda, A. Osuka, *J. Org. Chem.* **2001**, *66*, 8563–8572.

[18] Relative stabilities between NH tautomers of the basic frameworks in **2** and **3** may be essential factors: 7.78 and 4.72 kcal mol^{-1}, respectively, at the B3LYP/6–31G(d,p) level.[17]

[19] Errors are within 15%. The K_a values including errors are shown in the Supporting Figures.

[20] In [D_7]DMF, ^1H NMR signals of **2** and **3** resonate at $\delta = 0.53$ and ≈ 1.1 ppm for the inner CH and $\delta = 14.37$ and 13.88 ppm for the outer NH, respectively.

[21] Fluorescence change of NCTPP by F^- binding was reported briefly in reference [7a].

[22] J. P. Belair, C. J. Ziegler, C. S. Rajesh, D. A. Modarelli, *J. Phys. Chem. A* **2002**, *106*, 6445–6451.

[23] a) T. D. Lash, *Synlett* **2000**, 279–295; b) Z. Xiao, B. O. Patrick, D. Dolphin, *Chem. Commun.* **2002**, 1816–1817.

[24] *Gaussian 03*, Revision C.02, M. J. Frisch, G. W. Trucks, H. B. Schlegel, G. E. Scuseria, M. A. Robb, J. R. Cheeseman, J. A. Montgomery, Jr., T. Vreven, K. N. Kudin, J. C. Burant, J. M. Millam, S. S. Iyengar, J. Tomasi, V. Barone, B. Mennucci, M. Cossi, G. Scalmani, N. Rega, G. A. Petersson, H. Nakatsuji, M. Hada, M. Ehara, K. Toyota, R. Fukuda, J. Hasegawa, M. Ishida, T. Nakajima, Y. Honda, O. Kitao, H. Nakai, M. Klene, X. Li, J. E. Knox, H. P. Hratchian, J. B. Cross, C. Adamo, J. Jaramillo, R. Gomperts, R. E. Stratmann, O. Yazyev, A. J. Austin, R. Cammi, C. Pomelli, J. W. Ochterski, P. Y. Ayala, K. Morokuma, G. A. Voth, P. Salvador, J. J. Dannenberg, V. G. Zakrzewski, S. Dapprich, A. D. Daniels, M. C. Strain, O. Farkas, D. K. Malick, A. D. Rabuck, K. Raghavachari, J. B. Foresman, J. V. Ortiz, Q. Cui, A. G. Baboul, S. Clifford, J. Cioslowski, B. B. Stefanov, G. Liu, A. Liashenko, P. Piskorz, I. Komaromi, R. L. Martin, D. J. Fox, T. Keith, M. A. Al-Laham, C. Y. Peng, A. Nanayakkara, M. Challacombe, P. M. W. Gill, B. Johnson, W. Chen, M. W. Wong, C. Gonzalez, J. A. Pople, Gaussian, Inc., Wallingford CT, 2004.

[25] E. D. Glendening, A. E. Reed, J. E. Carpenter, F. Weinhold, NBO Version 3.1, Madison, WI, 1988.

[26] NPA charges of the complexes were shown in the Supporting Information.

[27] A direct comparison between **1–Cu** and **NCTPP–Cu** was extremely difficult because the latter phenyl derivative was too unstable for anion-binding studies.

[28] For the calculations, the basis-set superposition error and zero-point energy correction were not considered.[14c]

[29] Tris(pentafluorophenyl)-substituted NCPs **4–6** were prepared by [2+2] condensation of N-confused dipyrromethane derivatives and normal dipyrromethanes. See also reference [11].

[30] The data were analyzed by assuming a normal porphyrin structure, because the pyrrole groups in the crystal were disordered and only the 1/8 of the structure was available due to the symmetrical space group.
[31] The similar deprotonation of pyrrole NH by halide anions and the formation of ion-pair complexes was previously reported with 3,4-dichloro-2,5-diamidopyrroles: a) S. Camiolo, P. A. Gale, M. B. Hursthouse, M. E. Light, A. J. Shi, *Chem. Commun.* **2002**, 758–759; b) P. A. Gale, K. Navakhun, S. Camiolo, M. E. Light, M. B. Hursthouse, *J. Am. Chem. Soc.* **2002**, *124*, 11228–11229.
[32] M. Kakushima, P. Hamel, R. Frenette, J. Rokach, *J. Org. Chem.* **1983**, *48*, 3214–3219.

Received: June 6, 2006
Revised: August 8, 2006
Published online: November 8, 2006

